

# Histological Analysis of Benign Breast Imaging Reporting and Data System Categories 4c and 5 Breast Lesions in Imaging Study

Min Jung Kim,<sup>1</sup> Dokyung Kim,<sup>2</sup> WooHee Jung,<sup>2</sup> and Ja Seung Koo<sup>2</sup>

Departments of <sup>1</sup>Radiology, Research Institute of Radiological Science and <sup>2</sup>Pathology, Yonsei University College of Medicine, Seoul, Korea.

Received: September 26, 2011

Revised: October 31, 2011

Accepted: December 7, 2011

Corresponding author: Dr. Ja Seung Koo,  
Department of Pathology,  
Yonsei University College of Medicine,  
50 Yonsei-ro, Seodaemun-gu,  
Seoul 120-752, Korea.  
Tel: 82-2-2228-1772, Fax: 82-2-362-0860  
E-mail: kjs1976@yuhs.ac

The authors have no financial conflicts of interest.

**Purpose:** The objective of this study was to analyze the histology of breast lesions categorized as Breast Imaging Reporting and Data System (BI-RADS) 4c or 5 breast lesions during the imaging evaluation, but diagnosed as benign during the histological evaluation. **Materials and Methods:** We retrospectively reviewed 71 breast lesions categorized as BI-RADS 4c or 5 during imaging study, but diagnosed as benign upon histological evaluation. **Results:** Breast lesions were classified into six groups upon histological analysis: intraductal papilloma (18 cases), inflammatory group (15 cases), fibroepithelial tumor (14 cases), clustered microcalcification (10 cases), minimal histological alteration (10 cases), and adenosis (4 cases). Sclerosis and architectural complexity were associated with most of the biopsies that were morphologically similar to malignancy. **Conclusion:** Among 71 cases categorized as 4c or 5 during the imaging study, but diagnosed as benign upon histological examination, intraductal papilloma was the most frequently identified histological lesion. These 71 cases exhibited histological characteristics of sclerosis and/or complex/complicated features that should be histologically differentiated from malignancy during evaluation.

**Key Words:** Breast, biopsy, histology, breast imaging reporting and data system

## INTRODUCTION

Breast cancer is the most common cancer in women, the incidence of which continues to increase worldwide. Imaging screening has contributed to substantial reductions in breast cancer mortality, resulting in an increased prevalence of benign biopsies statistically.<sup>1-4</sup> Benign breast biopsies can be distressing, and therefore the correct interpretation of mammography and ultrasound (US) results for breast lesions is very important. The most commonly used interpretive criteria are drawn from the Breast Imaging Reporting and Data System (BI-RADS) recommended by the American College of Radiology.<sup>5</sup> BI-RADS classifies breast lesions from categories 2 to 5 depending on imaging characteristics as a final assessment, and category 4 is further subdivided into 4a, 4b, and 4c. In general, lesions of category 4 or category 5 are recommended for tissue biopsy. The percentages of cases diagnosed with breast cancer are 6% in category 4a, 15% in category 4b, 53% in category 4c, and 91% in category 5,<sup>6</sup> indicating that some benign breast lesions are initially wrongly interpreted as highly suspicious for malignancy. To our knowledge,

### © Copyright:

Yonsei University College of Medicine 2012

This is an Open Access article distributed under the terms of the Creative Commons Attribution Non-Commercial License (<http://creativecommons.org/licenses/by-nc/3.0>) which permits unrestricted non-commercial use, distribution, and reproduction in any medium, provided the original work is properly cited.

no studies on the histological analysis of breast lesions categorized as being of moderate concern for malignancy or worse (category 4c or 5) on US, but diagnosed as benign on histological examination have been reported. The purpose of this study was to analyze the histology of breast lesions categorized as 4c or 5 based on imaging, but diagnosed as benign on histological examination and to determine the implications thereof.

## MATERIALS AND METHODS

### Patient selection

We selected patients who had undergone breast US, breast core needle biopsy (CNB), and subsequent surgical excision between 2003 and 2010 and satisfied the following criteria for inclusion in the present study: 1) diagnosed as either BI-RADS category 4c or category 5 upon imaging study, including US and mammography (n=2385); 2) diagnosed as benign upon both breast US-guided CNB and subsequent surgical excision; and 3) lacking atypical ductal hyperplasia (ADH) or atypical lobular hyperplasia. This study included a total of 71 cases, and the Institutional Review Board (IRB) of Severance Hospital approved this study.

### Imaging study and biopsy protocol

Sonographically guided CNB was performed with a high-resolution sonographic unit and a 7.5- or 12-MHz linear array transducer (HDI 5000, Philips ATL; Logic 9, GE Healthcare, Bothell, WA, USA). All US imaging was performed by board-certified and breast-dedicated radiologists, and the final assessment of each US examination combined with mammographic information was analyzed prospectively by the same radiologists who performed the BI-RADS category based examination prior to biopsy.<sup>7</sup> For CNB, an automated gun (Pro-Mag 2.2, Manan Medical Products) and 14-gauge dual-action semiautomatic core biopsy needles (Stericut with coaxial; TSK Laboratory, Tochigi, Japan) were used. At the same time, the maximal dimension of the lesion was measured by US. CNB was performed by the same radiologists who performed the US, and 4-5 samples were obtained for each patient according to the standard protocol of our institute. These samples were submitted to the pathology department for histological examination. For each lesion that underwent CNB, imaging-histology correlations were reviewed at weekly conferences and the breast lesions with benign pathological biop-

sy results that were originally classified as category 4c or 5 were considered discordant lesions. Category 5 was defined for lesions with two or more major suspicious findings (irregular shape, spiculated margin, and microcalcification),<sup>8</sup> and non-category 5 lesions with a probability of malignancy greater than 80% were defined as category 4c.<sup>9</sup> Discordant lesions were recommended for excision. To generate the imaging descriptions for this study, one of the radiologists retrospectively reviewed all images according to the BI-RADS lexicon.<sup>10</sup> However, to prevent bias due to foreknowledge of the benign pathological diagnoses, we used the BI-RADS final assessment on the original radiology reports instead of re-categorizing the final assessment for the lesion.

### Histologic examination

All histological specimens were embedded in paraffin after fixation with 10% buffered formalin, sectioned at 4  $\mu$ m and stained with hematoxylin and eosin (H&E). The sections were examined by two pathologists (Koo JS and Kim D) using a light microscope. If needed, multiple serial sections were examined to detect microcalcification. Different results were discussed, and a consultation was made with a third pathologist when a persistent discordance occurred. When discrepancies between the pathological diagnosis of CNB and surgical excision were detected, the higher-level diagnosis was considered as the final diagnosis. For example, intraductal papilloma (IP) was taken as the final diagnosis if the case was diagnosed as IP by CNB and fibrocystic change by subsequent surgical excision. Immunohistochemical staining with p63 (DAKO, Glostrup, Denmark, 1 : 50, 4A4), estrogen receptor (ER, Thermo Scientific, San Jose, CA, USA, 1 : 100, SP1), and cytokeratin 5/6 (DAKO, Glostrup, Denmark, 1 : 100, D5/16B4) were performed if needed for diagnosis.

### Statistical analysis

Data were analyzed using Statistical Package for the Social Science (SPSS) software for Windows, version 12.0 (SPSS Inc., Chicago, IL, USA). Student's t-test and Fisher's exact test were used to analyze continuous and categorical variables, respectively. Statistical significance was assumed for *p*-values <0.05.

## RESULTS

### Radio-pathological features

Seventy-one cases were classified by histological analysis

into six groups: adenosis, clustered microcalcification (CMC), fibroepithelial tumor (FET), inflammatory group, intraductal papilloma (IP), and minimal histological alteration (MHA) (Table 1). Overall, IP was the most frequent diagnosis. There were 61 (85.9%) cases of category 4c lesions and 10 (14.1%) cases of category 5 lesions. IP was the most frequently identified lesion among the category 4c cases, and FET was the

most common lesion among the category 5 cases. The mean size of the breast lesions was 17.0±10.4 mm; the FET group had the largest mean size of 23.6±11.9 mm, and the adenosis group had the smallest mean size of 10.2±3.2 mm ( $p=0.057$ ).

Upon examination, all cases exhibited suspicious imaging findings, regardless of pathological grouping, indicative of 4c or 5 categorization. All 71 cases had non-circum-

**Table 1. Radiological Findings according to the Histological Groups of the 71 Cases of BI-RADS Category 4c or Category 5 Benign Breast Lesions**

Parameter	Total n=71 (%)	Histological group						p value
		Adenosis n=4 (%)	CMC n=10 (%)	FET n=14 (%)	Inflammatory n=15 (%)	IP n=18 (%)	MHA n=10 (%)	
<b>Mammographic finding*</b>								0.001
None	16 (25.8)	1 (6.3)	1 (6.3)	3 (18.8)	2 (12.5)	5 (31.3)	4 (25.0)	
Mass	31 (50.0)	2 (6.5)	1 (3.2)	9 (29.0)	8 (25.8)	6 (19.4)	5 (16.1)	
Calcification	12 (19.4)	0 (0.0)	8 (66.7)	0 (0.0)	1 (8.3)	2 (16.7)	1 (8.3)	
Mass and calcification	3 (4.8)	0 (0.0)	0 (0.0)	0 (0.0)	1 (33.3)	2 (66.7)	0 (0.0)	
<b>Ultrasonographic finding</b>								
<b>Shape</b>								0.078
Irregular	44 (62.0)	3 (6.8)	6 (13.6)	5 (11.4)	9 (20.5)	12 (27.3)	9 (20.5)	
Oval	20 (28.2)	0 (0.0)	2 (10.0)	9 (45.0)	4 (20.0)	4 (20.0)	1 (5.0)	
Round	7 (9.9)	1 (14.3)	2 (28.6)	0 (0.0)	2 (28.6)	2 (28.6)	0 (0.0)	
<b>Orientation</b>								0.487
Not-parallel	41 (57.7)	4 (9.8)	4 (9.8)	8 (19.5)	8 (19.5)	11 (26.8)	6 (14.6)	
Parallel	30 (42.3)	0 (0.0)	6 (20.0)	6 (20.0)	7 (23.3)	7 (23.3)	4 (13.3)	
<b>Margin</b>								0.012
Circumscribed	0 (0.0)	0 (0.0)	0 (0.0)	0 (0.0)	0 (0.0)	0 (0.0)	0 (0.0)	
Microlobulated	26 (36.6)	2 (7.7)	3 (11.5)	8 (30.8)	3 (11.5)	10 (38.5)	0 (0.0)	
Indistinct	14 (19.7)	0	3 (21.4)	4 (28.6)	5 (35.7)	0 (0.0)	2 (14.3)	
Angular	14 (19.7)	0 (0.0)	0 (0.0)	0 (0.0)	6 (42.8)	4 (28.6)	4 (28.6)	
Spiculated	17 (23.9)	2 (11.8)	4 (23.5)	2 (11.8)	1 (5.9)	4 (23.5)	4 (23.5)	
<b>Internal echogenicity</b>								0.169
Isoechoic	41 (59.1)	2 (4.9)	8 (19.5)	6 (14.6)	7 (17.1)	11 (26.8)	8 (19.5)	
Hypoechoic	29 (40.8)	2 (6.9)	2 (6.9)	8 (27.6)	8 (27.6)	7 (24.1)	2 (6.9)	
<b>Boundary</b>								0.136
Abrupt	46 (64.8)	3 (6.5)	9 (19.6)	11 (23.9)	6 (13.0)	11 (23.9)	6 (13.0)	
Echogenic halo	25 (35.2)	1 (4.0)	1 (4.0)	3 (12.0)	9 (36.0)	7 (28.0)	4 (16.0)	
<b>Posterior attenuation</b>								0.066
None	40 (56.3)	3 (7.5)	9 (22.5)	5 (12.5)	8 (20.0)	8 (20.0)	7 (17.5)	
Enhancement	17 (23.9)	0 (0.0)	0 (0.0)	6 (35.3)	3 (17.6)	8 (47.1)	0 (0.0)	
Shadowing	14 (19.7)	1 (7.1)	1 (7.1)	3 (21.4)	4 (28.6)	2 (14.3)	3 (21.4)	
<b>Microcalcification</b>								0.006
No	55 (77.5)	4 (7.3)	3 (5.5)	12 (21.8)	12 (21.8)	16 (29.1)	8 (14.5)	
Yes	16 (22.5)	0 (0.0)	7 (43.8)	2 (12.5)	3 (18.8)	2 (12.5)	2 (12.5)	
<b>Final assessment</b>								
Category 4c	61 (85.9)	3 (4.9)	9 (14.7)	11 (18.0)	13 (21.3)	17 (27.9)	8 (13.1)	
Category 5	10 (14.1)	1 (10.0)	1 (10.0)	3 (30.0)	2 (20.0)	1 (10.0)	2 (20.0)	
Size (mm, mean±SD)	17.0±10.4	10.2±3.2	11.5±4.9	23.6±11.9	16.6±6.3	13.1±5.3	18.5±16.1	0.057

CMC, clustered microcalcification; FET, fibroepithelial tumor; IP, intraductal papilloma; MHA, minimal histologic alteration; BI-RADS, Breast Imaging Reporting and Data System.

\*Sixty-two mammograms were available for review.

scribed margins. Non-parallel orientation was observed in 57.7% of the cases (41/71) and echogenic halo was observed in 21.1% of the cases (15/71). Irregular shape, spiculated margin, or microcalcification was observed in 70.4% of the cases (50/71). Microcalcifications on mammogram or sonogram were most frequently observed in the clustered microcalcification group than in the other groups ( $p < 0.05$ ). On radiology, 16 cases showed calcification, but 2 cases that belonged to the MHA group did not show microcalcification on histologic slides even after multiple serial sections.

### Histological characteristics

Four distinct histological characteristics were observed among 18 cases in the IP group. First, nine of these cases exhibited florid-type usual ductal hyperplasia (UDH) (Fig. 1A). Among the, 4 cases were able to be differentiated from a malignant papillary lesion by means of immunohistochemistry for p63 to confirm the presence of myoepithelial cells and for ER and CK5/6, which were negative and positive, respectively, indicative of UDH. Second, eight cases showed an entrapped and distorted gland/tubule structure in the sclerosing stroma (Fig. 1B). Among these, 2 cases were confirmed as benign duct/gland using immunohistochemistry for p63. Third, five cases showed slender papillary fronds rather than broad papillary fronds (Fig. 1C). Among these 5 cases, 2 cases were confirmed as benign papillary lesions using p63 stain to show myoepithelial cells in the papillary core. Lastly, there were two cases of complex sclerosing lesions, which showed a central area of stromal fibrosis with

entrapped and distorted glands, as well as both lobules and ducts, with somewhat radial configurations (Fig. 1D). These 2 cases were confirmed as benign lesions upon p63 staining, which revealed the presence of myoepithelial cells, and as UDH showed negativity for ER and positivity for CK5/6 stain. Four cases were diagnosed as adenosis with two histological characteristics. Two of these cases were sclerosing adenosis with glandular compression and distortion, accompanied by stromal proliferation, as the glands and tubules increased (Fig. 2A). Among the 4 cases, 2 cases were confirmed as benign ducts/glands using immunohistochemistry for p63. The remaining 2 cases showed extensive involvement of adenosis throughout the histological specimens, indicating diffuse involvement (Fig. 2B). CMC was observed in 10 cases, presenting calcifications of variable sizes clustered into groups in the intraluminal spaces of glands or tubules. Among these 10 cases, 6 cases showed CMC in cysts or normal terminal duct-lobular units, and 4 cases exhibited columnar cell change (Fig. 2C). In 5 cases, CMC was associated with ossifying-type calcification (OTC) that showed a central core of calcification with a rim of ossifying-type matrix (Fig. 2D). There were 14 cases with FET, nine with fibroadenoma and five with benign phyllodes tumor. Fibroadenoma exhibited three histological characteristics. The first was a sclerotic stromal component, which was observed in 5 cases (Fig. 3A). The sclerotic stromal component was observed throughout the whole lesion. Second, the epithelial component showed an intracanalicular pattern rather than a pericanalicular pattern in 5 cases (Fig. 3B). The intracanalicular pattern was similar in shape

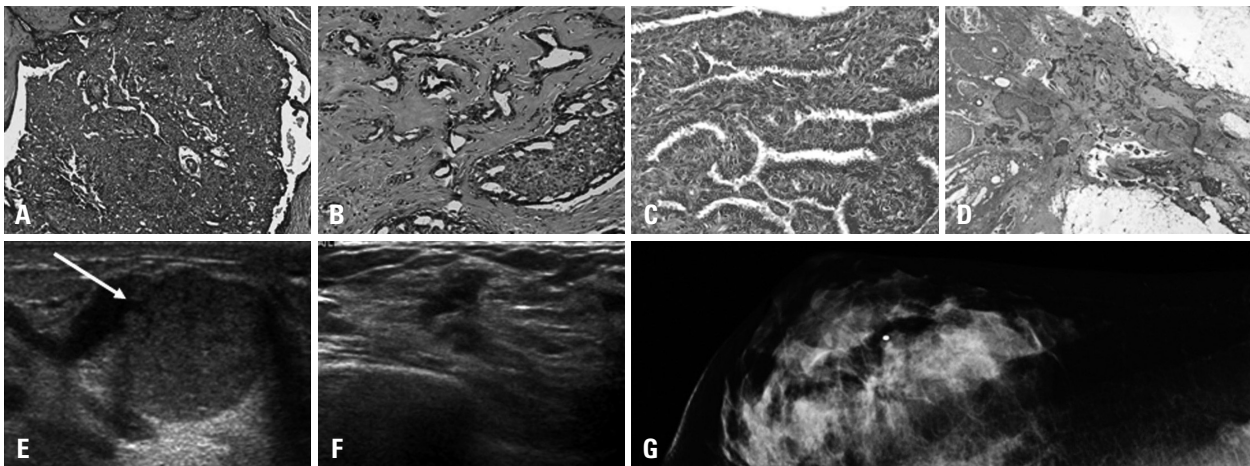


**Fig. 1.** Radiological and histological features of the IP group of category 4c or 5 lesions. The papilloma group showed histological features of florid-type usual ductal hyperplasia (A, H&E,  $\times 100$ ), entrapped and distorted glands in the sclerosing stroma (B, H&E,  $\times 100$ ), slender papillary fronds (C, H&E,  $\times 200$ ), and a complex sclerosing lesion with a stromal fibrosis zone with entrapped and distorted glands accompanying usual ductal hyperplasia and papilloma (D, H&E,  $\times 12$ ). IP with slender papillary fronds appeared as an intracystic isoechoic mass with a papillary frond (arrow) on ultrasonogram (E) and a complex sclerosing lesion appeared as a 1.0-cm sized irregular-shaped hypoechoic nodule with a spiculated margin and non-parallel orientation (F). The lateral view revealed a spiculated lesion (G). IP, intraductal papilloma.

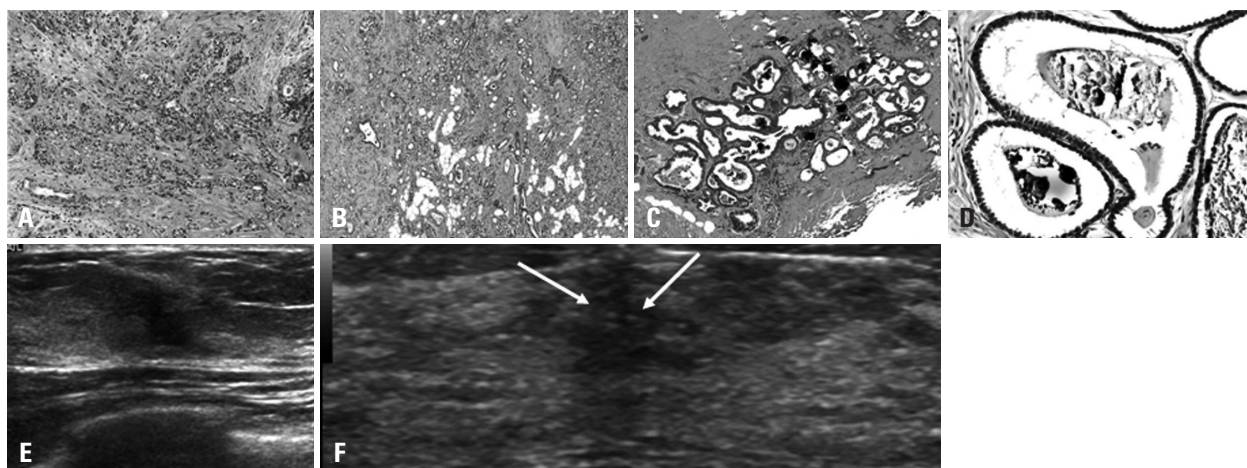


**Fig. 2.** Radiological and histological features of the adenosis and CMC groups of category 4c or 5 lesions. The adenosis group showed sclerosing adenosis (A, H&E,  $\times 100$ ), presenting as an irregularly spiculated hypoechoic mass on sonogram (E) and extensive involvement (B, H&E,  $\times 40$ ). CMC was observed in the intraluminal space of columnar cell change (C, H&E,  $\times 40$ ) and ossifying-type calcification showed central calcification with a rim of ossifying eosinophilic matrix (D, H&E,  $\times 200$ ), which appeared as echogenic foci (F, arrows) in a spiculated mass on sonogram. CMC, clustered microcalcification.

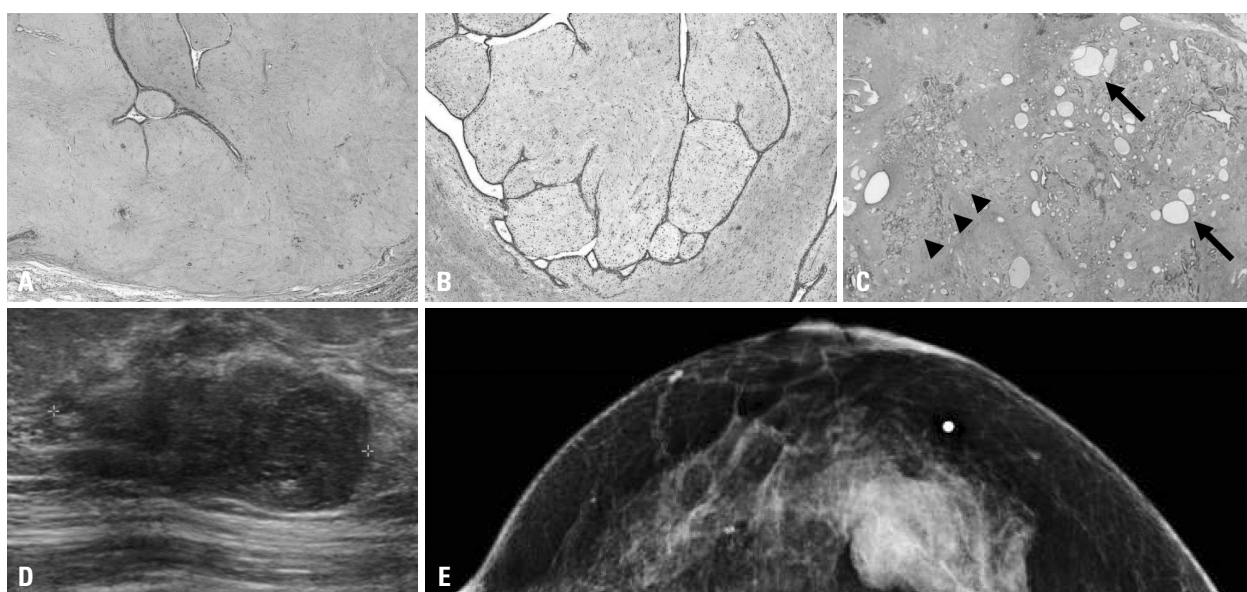


**Fig. 3.** Radiological and histological features of the fibroepithelial tumor group of category 4c or 5 lesions. Fibroadenoma demonstrated a sclerosing stromal component in the entire tumor lesion (A, H&E,  $\times 40$ ) and an intracanalicular growth pattern of the epithelial component (B, H&E,  $\times 40$ ). An oval microlobulated hypoechoic mass was observed on sonogram (D) and a hyperdense mass was observed on mammogram (E). Complex fibroadenoma showed variably sized cysts (arrow) and sclerosing adenosis (arrowhead) (C, H&E,  $\times 12$ ). CMC, clustered microcalcification.

to that of the epithelial component seen in phyllodes tumor. Lastly, two cases were complex fibroadenomas showing variable cystic structures with apocrine metaplasia and sclerosing adenosis (Fig. 3C). Fifteen cases belonged to the inflammatory group, which was the most heterogeneous group. Among these 15 cases, five showed fat necrosis with calcification or xanthogranulomatous inflammation (Fig. 4A). The other five cases showed complicated granulomatous lobular mastitis (GLM) complicated with abscess (Fig. 4B). Three cases were mammary duct ectasia with periductal sclerosis, lymphoplasmic cell infiltration, and duct distortion (Fig. 4C). The remaining two cases involved organizing thrombosis

and parasitic infection, respectively. Among 10 cases in the minimal histological alteration (MHA) group, six presented with stromal fibrosis (Fig. 5A) and the remaining 4 cases had normal breast tissue.

## DISCUSSION

In this study, histological analysis was performed on 71 cases of benign breast lesions that were categorized as BI-RADS 4c or 5 breast lesions based on imaging studies. Many studies on the differences between the results from imaging studies

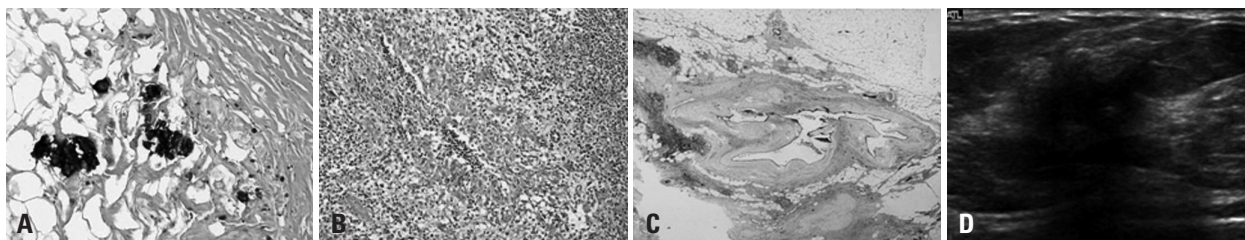


**Fig. 4.** Radiological and histological features of the inflammatory group of category 4c or 5 lesions. The inflammatory group demonstrated fat necrosis with calcification (A, H&E,  $\times 100$ ), granulomatous lobular mastitis complicated with abscess (B, H&E,  $\times 100$ ) and mammary duct ectasia showing an ecstatic duct, periductal sclerosis and lymphoplasmic cell infiltration (C, H&E,  $\times 12$ ), which appeared as an irregular, markedly hypoechoic mass with posterior shadowing on sonogram (D).

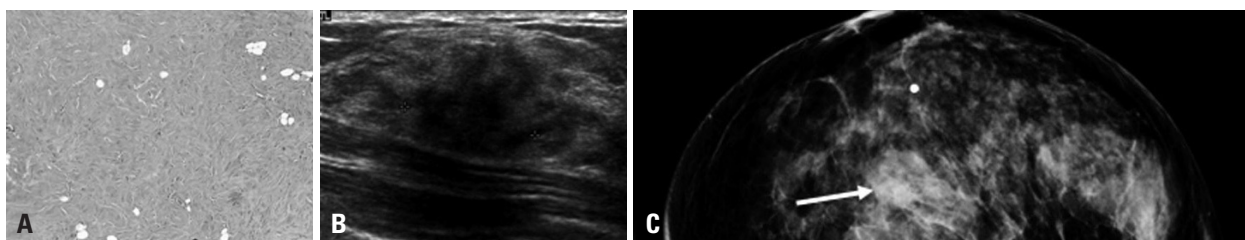


**Fig. 5.** Radiological and histological features of MHA of category 4c or 5 lesions. MHA did not show specific histological findings other than stromal fibrosis (A, H&E,  $\times 100$ ). The transverse sonogram showed an irregular microlobulated hypoechoic nodule with posterior shadowing (caliper, B), which was seen as an isodense mass on mammogram (arrow in C). MHA, minimal histological alteration.

and those from tissue examinations have been conducted. However, histological analyses of cases identified as false positives on imaging analysis have been rarely performed. A previous study reported that some cases interpreted as category 4, based on US, exhibited benign histological features of palpable or nonpalpable lesions.<sup>11</sup> The former showed fibroadenoma, epithelial and columnar cell hyperplasia, and lactating adenoma, while the latter included fibroadenoma, epithelial and columnar cell hyperplasia, and apocrine metaplasia.<sup>11</sup> In addition, the benign cases of category 5 lesions in that study were mucocele-like lesions with ADH, radial scars, and reactive nodes.<sup>11</sup> However, the previous study did not classify category 4 lesion into 4a, 4b, and 4c, as was done in this study. Because category 4a is seen more frequently in practice, results for category 4c alone might be obscured. The previous study also only investigated the results of CNB, not CNB and subsequent surgical excision, as was done in this study. Therefore, a comparison of previous results with the results of this study may not be reasonable. In this study, the possibility that a malignant lesion was not sampled was probably low, because we included only the cases diagnosed as benign on both CNB and subsequent surgical excision.

Based on a review of previous literature, irregular shape, such as spiculated, microlobulated, or angular margin microcalcifications, nonparallel orientation, echogenic halo, ductal extension, hypoechogenicity or complex echogenicity, and posterior shadowing have all been considered as

suspicious US features.<sup>8,10,12</sup> In the study of Kim, et al.,<sup>8</sup> suspicious findings were divided into major findings, such as irregular shape, spiculated margin and microcalcifications, and minor findings, such as round shape, microlobulated/indistinct/angular margins, nonparallel orientation, duct extension, complex echogenicity, and posterior shadowing. Kim, et al.<sup>8</sup> recommended defining the final assessment according to the number of major or minor suspicious findings shown; category 5 lesions were defined as lesions showing two or more major suspicious features and category 4c lesions included lesions with one major suspicious feature, with or without minor suspicious features. Additionally, they advised against basing the final assessment on imaging findings alone.<sup>10</sup> However, there are still no widely accepted guidelines for concluding the final assessment or for identifying findings that would cause a lesion to be classified into a certain category. The first reason for mismatching between radiology and histology is that clinical information such as age, personal history, multiplicity, and symptoms should be considered because such information may affect radiologist's decisions for categorization of breast lesion.<sup>9,13</sup> In this study, nearly 70% of the cases considered to be of category 4c or 5 had at least one of the major suspicious findings suggested by Kim, et al.<sup>8</sup> The remaining 30% of the category 4c or 5 cases had at least one minor suspicious finding, such as symptoms, personal cancer history, or patient age. A second potential reason for mismatching between radiology and histology guideline is

interobserver variability, which has a known kappa value of 0.28-0.80 for final assessments and lexicons.<sup>14,15</sup> The imaging findings were retrospectively reviewed by one experienced radiologist. The only way to verify the propriety of the final assessment is performing a medical audit on each radiologist and each imaging center, which was not performed in this study. The appropriate positive predictive value was considered to be greater than 50% for category 4c and greater than 95% for category 5, and the percentage of benign lesions actually classified into categories 4c and 5 in this study was around 7% (71/2385), which is within the previously reported range.<sup>14,15</sup>

In this study, cases were classified into six histological groups (adenosis, CMC, FET, inflammatory, IP and MHA), exhibiting three characteristic histological features. First was a sclerosing or fibrosing feature that we observed in the following lesions: sclerosing adenosis in the adenosis group, sclerosis of the stromal component of fibroadenomas and sclerosing adenosis of complex fibroadenomas in the FET group, periductal sclerosis of mammary duct ectasia in the inflammatory group, entrapped/distorted glands of sclerotic stroma in the IP group, a sclerotic stromal zone of complex sclerosing lesions in the IP group, and stromal fibrosis in the MHA group. Unfortunately, there have not been enough studies to examine how sclerosis of the breast impacts US imaging. In a previous study, images of cases diagnosed as focal fibrosis on US-guided CNB originally belonged to category 3 or category 4a.<sup>16</sup> A comparison of this previous study with our study is not appropriate, as sclerosis in the previous study had diffuse involvement rather than focal involvement and was also accompanied by underlying breast disease. Such sclerosis could distort underlying breast lesions or structures, resulting in suspicious lesions on imaging studies. The second histological feature included complex or complicated features that were found in the following lesions: complex fibroadenoma in the FET group, complicated GLM with abscess and mammary duct ectasia (ectatic duct, periductal sclerosis, lymphoplasmic cell infiltration) in the inflammatory group, and complex sclerosing lesion in the IP group. Such histologically complex lesions could be interpreted as malignancies on imaging studies. The image findings for complex fibroadenoma include cystic changes or calcifications rather than typical fibroadenomas with elliptical, well-defined margins.<sup>17</sup> However, it has been reported that GLMs appear as suspicious cancers on mammography and “multiple clustered, often contiguous tubular hypoechoic lesions” on US.<sup>18</sup> Also,

mammary duct ectasia may mimic cancer on mammography.<sup>19</sup> In addition, the complex sclerosing lesions in the radial scar group appeared less organized than typical radial scars and could represent a late stage of sclerosing papilloma.<sup>20</sup> It has been reported that a radial sclerosing lesion can mimic carcinoma on imaging analysis.<sup>21,22</sup> Third, there are the histological features that should be differentiated from malignancy. Sclerosing adenosis in the adenosis group showed compressed and distorted glands by stromal proliferation, mimicking invasive ductal carcinoma (IDC). In such situations, immunohistochemical staining with markers such as p63 to detect myoepithelial cells can aid in differential diagnosis.<sup>20</sup> In this study, IP with florid-type UDH was presented in the IP group. When IP involves an area of ductal cell proliferation, such as florid-type UDH, IP with ADH or IP with ductal carcinoma *in situ* (DCIS) becomes the main differential diagnosis.<sup>20</sup> For papillary lesions that are difficult to diagnose, it is necessary to examine the expression patterns of cytokeratin 5/6 and ER in the ductal cell proliferation area, which are helpful for differential diagnosis. Cytokeratin 5/6 is expressed and ER is not expressed in IP with florid-type UDH, while cytokeratin 5/6 is not expressed and ER is expressed in IP with ADH or IP with DCIS.<sup>23-26</sup> As, histological features of entrapped and distorted glands in the sclerotic stroma in the IP group are similar to those in IDC, the use of a myoepithelial cell marker such as p63 can aid in differential diagnosis, as in the case of sclerosing adenosis.<sup>20</sup> Slender papillary fronds were observed in the IP group in this study. In general, benign papillomas have wider papillary fronds than papillary carcinomas.<sup>20</sup> The confirmation of continuous myoepithelial cells in the papillary core by immunohistochemical staining such as p63 helps when a benign papilloma shows slender papillary fronds.<sup>25</sup>

In this study, OTC was observed in 5 of 10 cases of CMC. OTC does not actually contain osteocytes or osteoblasts, but is morphologically similar to osseous tissue on H&E stained slides.<sup>27,28</sup> OTC can be found across the entire spectrum of proliferative duct lesions. However, studies of the radiological appearance of OTC are rare. Further study is needed to clarify two conflicting opinions: 1) OTC cannot be differentiated from other types of calcification,<sup>27</sup> and 2) OTC appears as dense cluster on radiological analysis.<sup>28</sup>

In conclusion, based on our analysis of 71 cases that were categorized as 4c or 5 on imaging analysis but were then diagnosed as benign on histological examination, we found that IP was the most commonly identified lesion, followed

by the inflammatory group, FET, CMC MHA, and adenosis, in that order. The distinguishing histological characteristics of these six groups were sclerosis and architectural complexity indicative of malignancy.

## ACKNOWLEDGEMENTS

This work was supported by Yonsei University Research Fund of 2011.

## REFERENCES

- Buchberger W, DeKoekoek-Doll P, Springer P, Obrist P, Dünser M. Incidental findings on sonography of the breast: clinical significance and diagnostic workup. *AJR Am J Roentgenol* 1999;173:921-7.
- Poplack SP, Tosteson AN, Grove MR, Wells WA, Carney PA. Mammography in 53,803 women from the New Hampshire mammography network. *Radiology* 2000;217:832-40.
- Berg WA, Blume JD, Cormack JB, Mendelson EB, Lehrer D, Böhm-Vélez M, et al. Combined screening with ultrasound and mammography vs mammography alone in women at elevated risk of breast cancer. *JAMA* 2008;299:2151-63.
- Houssami N, Lord SJ, Ciatto S. Breast cancer screening: emerging role of new imaging techniques as adjuncts to mammography. *Med J Aust* 2009;190:493-7.
- Obenauer S, Hermann KP, Grabbe E. Applications and literature review of the BI-RADS classification. *Eur Radiol* 2005;15:1027-36.
- Lazarus E, Mainiero MB, Schepps B, Koelliker SL, Livingston LS. BI-RADS lexicon for US and mammography: interobserver variability and positive predictive value. *Radiology* 2006;239:385-91.
- Mendelson E, Baum J, Berg W, Merritt C, Rubin E. *Ultrasound*. In: *Breast Imaging Reporting and Data System (BI-RADS)*. 4th ed. Reston, VA: American College of Radiology; 2003.
- Kim EK, Ko KH, Oh KK, Kwak JY, You JK, Kim MJ, et al. Clinical application of the BI-RADS final assessment to breast sonography in conjunction with mammography. *AJR Am J Roentgenol* 2008;190:1209-15.
- Yoon JH, Kim MJ, Moon HJ, Kwak JY, Kim EK. Subcategorization of ultrasonographic BI-RADS category 4: positive predictive value and clinical factors affecting it. *Ultrasound Med Biol* 2011;37:693-9.
- ACR BI-RADS, breast imaging and reporting data systems: breast imaging atlas; mammography, breast ultrasound, magnetic resonance imaging. Reston, VA: American College of Radiology; 2003.
- Raza S, Chikarmane SA, Neilsen SS, Zorn LM, Birdwell RL. BI-RADS 3, 4, and 5 lesions: value of US in management–follow-up and outcome. *Radiology* 2008;248:773-81.
- Stavros AT, Thickman D, Rapp CL, Dennis MA, Parker SH, Sisney GA. Solid breast nodules: use of sonography to distinguish between benign and malignant lesions. *Radiology* 1995;196:123-34.
- Baek SE, Kim MJ, Kim EK, Youk JH, Lee HJ, Son EJ. Effect of clinical information on diagnostic performance in breast sonography. *J Ultrasound Med* 2009;28:1349-56.
- Lee HJ, Kim EK, Kim MJ, Youk JH, Lee JY, Kang DR, et al. Observer variability of Breast Imaging Reporting and Data System (BI-RADS) for breast ultrasound. *Eur J Radiol* 2008;65:293-8.
- Park CS, Lee JH, Yim HW, Kang BJ, Kim HS, Jung JI, et al. Observer agreement using the ACR Breast Imaging Reporting and Data System (BI-RADS)-ultrasound, First Edition (2003). *Korean J Radiol* 2007;8:397-402.
- You JK, Kim EK, Kwak JY, Kim MJ, Oh KK, Park BW, et al. Focal fibrosis of the breast diagnosed by a sonographically guided core biopsy of nonpalpable lesions: imaging findings and clinical relevance. *J Ultrasound Med* 2005;24:1377-84.
- Stavros A. *Breast Ultrasound*. Philadelphia: Lippincott Williams & Wilkins; 2004.
- Han BK, Choe YH, Park JM, Moon WK, Ko YH, Yang JH, et al. Granulomatous mastitis: mammographic and sonographic appearances. *AJR Am J Roentgenol* 1999;173:317-20.
- Sweeney DJ, Wylie EJ. Mammographic appearances of mammary duct ectasia that mimic carcinoma in a screening programme. *Australas Radiol* 1995;39:18-23.
- Schnitt SJ, Collins LC. *Biopsy Interpretation of the Breast*. 1st ed. New York: Lippincott Williams & Wilkins; 2009.
- Mitnick JS, Vazquez MF, Harris MN, Roses DF. Differentiation of radial scar from scirrhous carcinoma of the breast: mammographic-pathologic correlation. *Radiology* 1989;173:697-700.
- Adler DD, Helvie MA, Oberman HA, Ikeda DM, Bhan AO. Radial sclerosing lesion of the breast: mammographic features. *Radiology* 1990;176:737-40.
- Shah VI, Flowers CI, Douglas-Jones AG, Dallimore NS, Rashid M. Immunohistochemistry increases the accuracy of diagnosis of benign papillary lesions in breast core needle biopsy specimens. *Histopathology* 2006;48:683-91.
- Ichihara S, Fujimoto T, Hashimoto K, Moritani S, Hasegawa M, Yokoi T. Double immunostaining with p63 and high-molecular-weight cytokeratins distinguishes borderline papillary lesions of the breast. *Pathol Int* 2007;57:126-32.
- Tse GM, Tan PH, Lui PC, Gilks CB, Poon CS, Ma TK, et al. The role of immunohistochemistry for smooth-muscle actin, p63, CD10 and cytokeratin 14 in the differential diagnosis of papillary lesions of the breast. *J Clin Pathol* 2007;60:315-20.
- Grin A, O'Malley FP, Mulligan AM. Cytokeratin 5 and estrogen receptor immunohistochemistry as a useful adjunct in identifying atypical papillary lesions on breast needle core biopsy. *Am J Surg Pathol* 2009;33:1615-23.
- Resetskova E, Hoda SA. "Ossifying-type" mammary calcifications. *Arch Pathol Lab Med* 2002;126:995-6.
- Hoda SA, Gopalan A. Mammary calcifications of the ossifying type. *Breast J* 2003;9:129-30.